IOP Conf. Series: Journal of Physics: Conf. Series **1023** (2018) 012019 doi:10.1088/1742-6596/1023/1/012019

Low collectivity of the first 2^+ states of ^{212,210}Po

D. Kocheva[1], G. Rainovski[1], J. Jolie[2], N. Pietralla[3], A. Blazhev[2], A. Astier[4], R. Altenkirch[2], M. Bast[2], M. Beckers[2], S. Ansari[2], Th. Braunroth[2], M. Cappellazzo[2], M.L. Cortés[3], A. Dewald[2], F. Diel[2], M. Djongolov[1], C. Fransen[2], K. Gladnishki[1], A. Goldkuhle[2], A. Hennig[2], V. Karayonchev[2], J.M. Keatings[5], E. Kluge[2], Th. Kröll[3],J. Litzinger[2], K. Moschner[2], C. Müller-Gatermann[2], P. Petkov[6], M. Rudigier[2], M. Scheck[5], P. Spagnoletti[5], Ph. Scholz[2], T. Schmidt[2], M. Spieker[2], C. Stahl[3], R. Stegmann[3], A. Stolz[2], A. Vogt[2], M. Stoyanova[1], P. Thöle[2], N. Warr[2], V. Werner[3], W. Witt[3], D. Wölk[2], J.C. Zamora[3], K.O. Zell[2], P. Van Isacker[7], V.Yu. Ponomarev[3]

[1] Faculty of Physics, St. Kliment Ohridski University of Sofia, 1164 Sofia, Bulgaria
[2] Institut für Kernphysik, Universität zu Köln, 50937 Cologne, Germany
[3] Institut für Kernphysik, Technische Universität Darmstadt, 64289 Darmstadt, Germany
[4] CSNSM, IN2P3/CNRS and Universite Paris-Sud, F-91405 Orsay Campus, France
[5] University of the West of Scotland, PA1 2BE Paisley, UK and SUPA, Glasgow G12 8QQ, UK
[6] National Institute for Physics and Nuclear Engineering,77125 Bucharest-Magurele, Romania
[7] Grand Accélérateur National d'Ions Lourds, CEA/DRF-CNRS/IN2P3, Bd. Henri Becquerel BP 55027, F-14076 Caen, France

E-mail: dkocheva@phys.uni-sofia.bg

Abstract. The lifetimes of the first 2^+ excited states of ^{212,210}Po were measured in two transfer reactions ^{208}Pb(^{12}C,^{8}Be)^{212}Po and ^{208}Pb(^{12}C,^{10}Be)^{210}Po by the Recoil Distance Doppler Shift (RDDS) method and by the Doppler Shift Attenuation method (DSAM), respectively. The derived absolute $B(E2)$ values of 2.6(3) W.u. for ^{212}Po and 1.83(28) W.u. for ^{210}Po indicate low collectivity. It is shown that the properties of the yrast 2_1^+, 4_1^+, 6_1^+ and 8_1^+ states in both nuclei cannot be described consistently in the framework of nuclear shell models. It is also demonstrated in the case of ^{210}Po that Quasi-particle Phonon Model (QPM) calculations cannot overcome this problem thus indicating the existence of a peculiarity which is neglected in both theoretical approaches.

1. Introduction

Understanding nuclear structure in terms of single-particle motion and collective behaviour is one of the challenges of nuclear physics. The nuclear shell model provides the basic framework for understanding of the single-particle motion in nuclei [1].The collective behaviour is understood as a result of coherent movement of valence nucleons caused by the residual interaction [2]. In this regard, properties of open-shell nuclei in the immediate vicinity of double-magic cores are of particular importance. Such nuclei can often be understood well within the framework of the shell models and at the same time their valence particles can induce the onset of collective behaviour. With two and four valence nucleons in respect to the double-magic core ^{208}Pb the

nuclei ^{210}Po and ^{212}Po provide a good testing ground for studying the beginning of the evolution from single-particle to collective motion in the mass $A \approx 208$ region.

In a recent study, it has been shown that a phenomenological single-j shell model accounts very well for the energies of the low-lying states of ^{212}Po (cf. Fig. 3 in Ref. [3]). In addition, Auerbach and Talmi [4] have suggested that the yrast sequence $2_1^+ - 4_1^+ - 6_1^+ - 8_1^+$ of ^{212}Po follows a seniority-like energy pattern resulting in an isomeric 8_1^+ state. All of this raises the question whether shell models can describe consistently the electromagnetic properties of the $2_1^+ - 4_1^+ - 6_1^+ - 8_1^+$ sequence as well. To address these questions experimental information on the absolute $B(E2)$ strengths for the $4_1^+ \rightarrow 2_1^+$ and $2_1^+ \rightarrow 0_1^+$ transitions is needed.

In the case of ^{210}Po, data on its absolute strengths for $E2$ transitions between its yrast states are available [5, 6]. Large-scale shell-model studies of ^{210}Po using realistic interactions [7, 8] well reproduce the energies of the yrast 2^+, 4^+, 6^+, and 8^+ levels. The $E2$ strengths for the transitions between the 4^+, 6^+ and 8^+ states are also almost perfectly reproduced (cf. Table VII in Ref. [7] and Table III in Ref. [8]). However, in both studies [7, 8] the $B(E2; 2_1^+ \rightarrow 0_1^+)$ value is overestimated by a factor of six. Such a significant discrepancy between the shell-model calculations and the data is an indication for either an inaccurate experimental value [7, 8] or for deficiencies in the model, as suggested in Ref. [8].

All of this has motivated us to perform two experiments especially designed to measure the lifetimes of the 2_1^+ states of ^{212,210}Po. Both experiments were performed at the FN Tandem facility at the University of Cologne, Germany.

2. Lifetime measurement of the first 2^+ state of ^{212}Po

2.1. Experimental set-up

The lifetime of the 2_1^+ state of ^{212}Po was measured by utilizing the RDDS method [9, 10]. The excited states of ^{212}Po were populated using the α-transfer reaction ^{208}Pb(^{12}C,^{8}Be)^{212}Po. The target consisted of a 0.6 mg/cm^2 thin layer of Pb evaporated on a 2 mg/cm^2 thick Au backing foil and was placed with the Au facing the beam. The beam energy of 64 MeV was chosen in such a way that the energy at which the reaction takes place after the Au backing to be about $\sim$ 62 MeV. The reaction was induced in the reaction chamber of the Cologne coincidence plunger device [11]. The stopper was a self-supporting 2 mg/cm^2 thick Au foil. Data were taken at six plunger distances: 25μm, 35μm, 43μm, 55μm, 70μm and 100μm.

For detecting the light reaction fragments six solar cells (10 mm $\times$ 10 mm) were used. The array of solar cells was mounted in the plunger chamber at backward angles with respect to the beam axis, covering an angular range between 116.8° and 167.2°. The solar cells were placed at a distance of about 15 mm between their centres and the target. The γ rays from the decay of the excited states of ^{212}Po were registered by 11 HPGe detectors mounted outside the plunger chamber in two rings at distance of, on average, 12 cm from the target. Five detectors were positioned at backward angles (142° with respect to the beam axis) and the other six detectors were placed at forward angles (45° with respect to the beam axis). Data were taken in coincidence mode of at least one solar cell and one HPGe detector (particle-γ) or when at least two HPGe detectors (γ-γ) were in coincidence.

2.2. Data analysis and results

The particle-γ coincidence data were sorted in twelve matrices depending on the positions of the HPGe detectors and the plunger distances. A particle projection of the particle-γ matrix is shown in Fig. 1(a) as an example. The γ rays in coincidence with the group of particles indicated as "^{212}Po & ^{200}Tl" in Fig. 1(a) are shown in Fig. 1(b). This spectrum is dominated by transitions from excited states of ^{200}Tl which is produced by the ^{197}Au(^{12}C,2αn) transfer reaction in the backing or in the stopper. However, the 727-, 405-, and 223-keV lines which are the γ-ray transitions depopulating the first three yrast states of ^{212}Po [12, 13, 3] are also clearly

visible. Moreover, it is also visible from Fig. 2 (a) that the 727-keV transition between the 2_1^+ state of ^{212}Po and its ground state, has a well pronounced shifted component which evolves as a function of plunger distance.

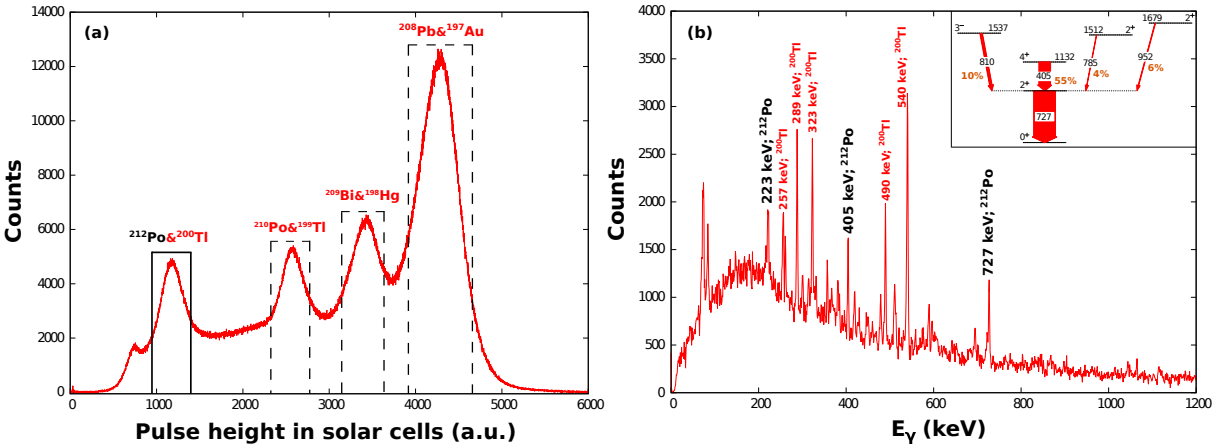

Figure 1. (Color online) (a) The projection of the particle-γ matrix obtained at plunger distance (D=43 μm) by coincident detection of charged particles in the solar-cell array and γ rays at a polar angle $\Theta_\gamma = 142°$. The marked ranges represent parts of the particle spectrum found to be in coincidence with the γ rays from the indicated nuclei. (b) The γ-ray spectrum in coincidence with the group of particles indicated as "^{212}Po & ^{200}Tl" in panel (a). (inset) Partial level scheme of ^{212}Po showing the excited states which feed the first excited 2^+ state directly. The thicknesses of the arrows (and the shown percentages) are proportional to the observed γ -ray intensities [14].

The RDDS data for this transition was analysed by utilizing the Differential Decay Curve Method (DDCM) [15, 16]. The standard application of DDCM requires the I_γ^{sh} and I_γ^{un} components (for each distance) to be measured from spectra in coincidence with Doppler-shifted components of transitions that feed directly the excited state of interest. Then the lifetime τ_i of the level of interest for the i-th target-to-stopper distance depends on I_{sh} and I_{un} in the simple way [15, 16]:

$$\tau_i(x) = \frac{I_{un}(x)}{\langle v \rangle \frac{d}{dx} I_{sh}(x)} \tag{1}$$

as here the derivative of the Doppler shifted intensities as a function of the target-to-stopper distance, $\frac{d}{dx} I_{sh}$, is determined by a piecewise polynomial fit to the measured intensities I_{sh}.

The presented particle-gated γ-ray spectra in Fig. 2(a) are, in fact, γ-ray singles spectra which, in principal, only contain information for the effective lifetime of the 2_1^+ state of ^{212}Po. Therefore, the intensities of the I_{sh} and I_{un} derived from these spectra cannot be used directly for extracting the lifetime of the 2_1^+ state by means of the DDCM. Special care has to be taken into account for analyzing the impact of the transitions directly feeding the 2_1^+ state on the I_{sh} and I_{un} components of the 727-keV transition (see the inset in Fig. 1(b)).

The lifetimes of the $2_{2,3}^+$ states of ^{212}Po were measured in our previous study [3] to be below 1 ps which means that they contribute only to the fast feeding of the 2_1^+ state. The lifetime of the 3^- state at 1537 keV is not known and in order to simplify the discussion at this moment we assume that its lifetime is sufficiently short so that it decays only in flight. Under this assumption the only essential feeder to the 2_1^+ state remains the 405-keV transition which depopulates the 4_1^+ state of ^{212}Po. It is expected that the 4_1^+ state has a long lifetime of about 140 ps, or longer [3]. Indeed, as can be seen from the insets in Fig. 2(a) the 405-keV transition has only a stopped component for all plunger distances, *i.e.* the decay of the 4_1^+ state contributes

IOP Conf. Series: Journal of Physics: Conf. Series **1023** (2018) 012019 doi:10.1088/1742-6596/1023/1/012019

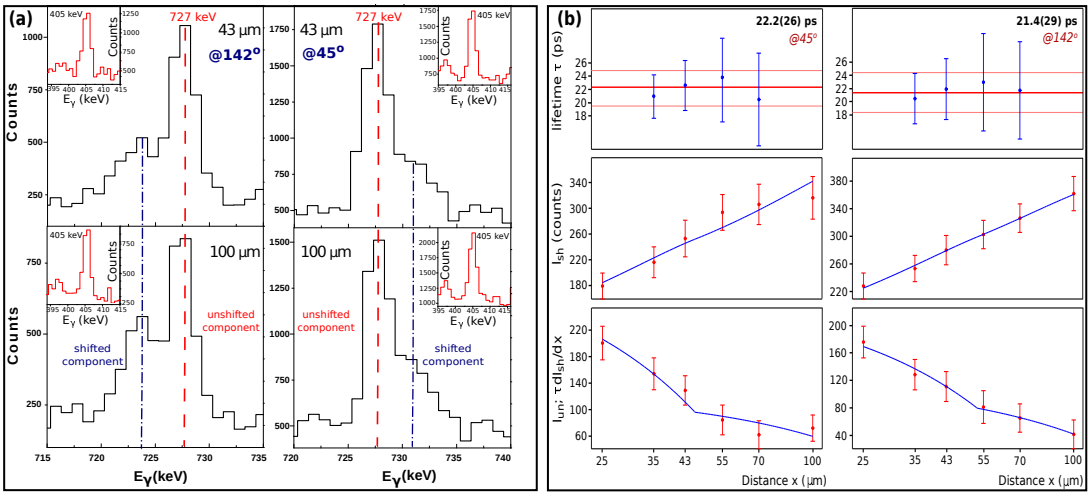

Figure 2. (Color online) (a) Examples of the evolution of the intensities of the Doppler shifted peaks of the 727-keV ($2_1^+ \rightarrow 0_1^+$) transition observed at backward angles and at forward angles for two different target-to-stopper distances. The dot-dashed lines (blue) represent the positions of the Doppler-shifted peak; the dashed lines (red) represent the unshifted peak positions. At the upper corners are shown the peaks of the 405-keV ($4_1^+ \rightarrow 2_1^+$) transition at the same detector angle and distance as those for the $2_1^+ \rightarrow 0_1^+$ transition. (b) The lifetime of the first excited 2^+ state of ^{212}Po determined at forward and backward angles. The middle panels show the shifted intensities at different distances. Continuous curves are fitted through the points to calculate the derivative. In the bottom panels, curves that represent the product between the time derivatives of the shifted intensities and the lifetime of the level are compared with the experimental unshifted intensities. Out of this comparison, the lifetimes corresponding to each distance in the region of sensitivity are extracted, as seen in the upper panel. The horizontal lines represent the weighted mean values.

only to the stopped component of the 727-keV transition. Hence, that extra contribution to the stopped component of the 727-keV transition has to be eliminated. In our analysis this was achieved by subtracting the efficiency-corrected number of counts in the 405-keV line out of the efficiency-corrected number of counts in the stopped component of the 727-keV transition (cf. Fig. 2(a)). Under the considerations above, it is obvious that the intensities of the shifted components of the 727-keV transition being directly determined from the particle-gated spectra are also related only to the lifetime of the 2_1^+ state of ^{212}Po. In this respect, both I_γ^{un} and I_γ^{sh} can be considered as effectively derived from γ-ray spectra in coincidence with the shifted components of all transitions directly feeding the state of interest. Therefore, they can be used directly in Eq. (1).

To proceed with the DDCM analysis the mean velocity of the recoiling nuclei $\langle v \rangle$ has to be known. This value was experimentally determined from the centroids of the shifted and the unshifted components of 727-keV transition to be $\langle v \rangle$ =0.72(5)%c. The DDCM fits using $\langle v \rangle$ =0.72(5)%c and intensities (I_γ^{un} and I_γ^{sh}) extracted with the procedure described above are shown in Fig. 2(b). These fits result in a weighted mean value for the lifetime of the 2_1^+ state of 21.8(19) ps.

It has to be noted that the only assumption in the derivation of the above result which is not directly supported by experimental observations, is that the feeding from the 3_1^- state is fast. To investigate the influence of this feeding to the lifetime of the 2_1^+ state further, we have also considered the alternative limit, *i.e.* we have assumed that the feeding from the 3_1^- state is very slow and contributes only to the unshifted component of the 727-keV transition. In this case, besides the intensity of the 405-keV transition, the intensity of the

unshifted component of the 727-keV transition has to be reduced by additional 10% which accounts for the intensity of the 810-keV transition ($3_1^- \rightarrow 2_1^+$, cf. the inset of Fig. 1(b)). This alternative approach reduces the deduced lifetime of the 2_1^+ to 19.2(18) ps. For the final value for the lifetime of the 2_1^+ state we conservatively adopt the average value between the two limits which is: $\tau(2_1^+, E_x = 727\ \mathrm{keV}) = 20.5(26)$ ps. Taking into account the known electron conversion coefficient for the $2_1^+ \rightarrow 0_1^+$ transition of ^{212}Po [12] and α-branching ratio [13], the newly derived lifetime of the 2_1^+ state translates to absolute transition strength $B(E2; 2_1^+ \rightarrow 0_1^+) = 193(24)$ $\mathrm{e^2fm^4} = 2.6(3)$ Wu.

3. Lifetime measurement of the first 2^+ state of ^{210}Po

3.1. Experimental set-up

For measuring the lifetime of the first 2^+ state of ^{210}Po by means of DSAM (cf. Ref. [9] and references therein) the ^{208}Pb(^{12}C,^{10}Be)^{210}Po transfer reaction was used. The target was a self-supporting 10 mg/cm^2 thick Pb foil enriched to 99.14 % with the isotope ^{208}Pb. Besides the placement of the ring at forward angles at 35°, the experiment was performed with the same detectors' set-up as the previous one.

3.2. Data analysis and results

The particle-γ coincidence data were sorted in two matrices depending on the position of the HPGe detectors. A projection of the particle-γ matrix obtained with γ-ray detection at 142.3° is shown in Fig. 3(a). The γ rays in coincidence with the group of particles indicated as "^{210}Po" in Fig. 3(a) are shown in Fig. 3(b). This spectrum is dominated by the 1181-keV and the 245-keV lines which are the γ-ray transitions depopulating the first two yrast states of ^{210}Po [17]. Besides some contaminants from ^{211}Po (which are shown in purple), all other γ rays originate from the decay of excited states of ^{210}Po. The 1181-keV γ-ray line shows Doppler shape which allow us to extract the lifetime of the 2_1^+ state of ^{210}Po (cf. Fig 4).

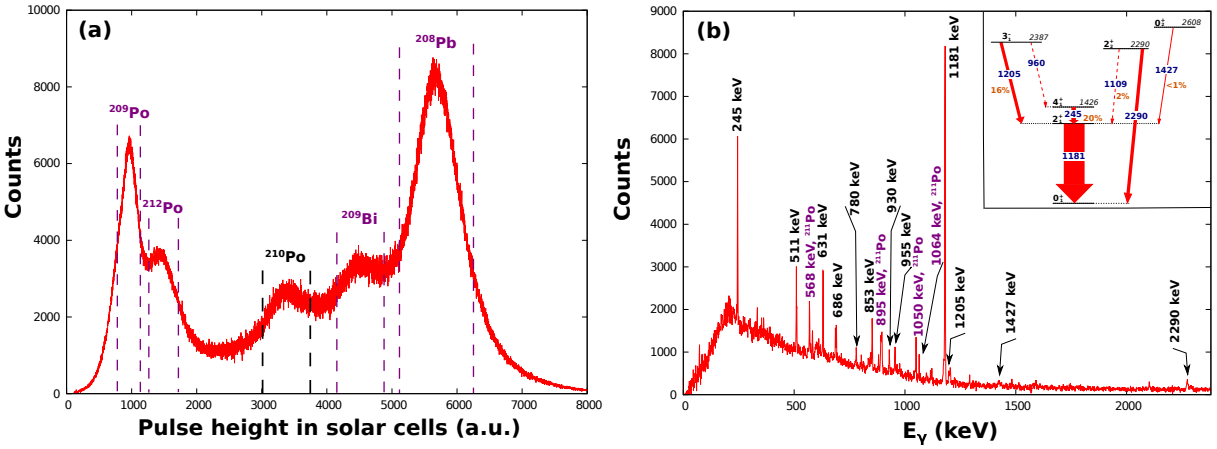

Figure 3. (Color online) (a) The projection of the particle-γ matrix obtained by coincidence detection of charged particles in the solar-cell array and γ rays at $\Theta_\gamma = 142°$ polar angle. The vertical dashed lines represent parts of the particle spectrum found to be in coincidence with γ rays from the indicated nuclei. (b) The γ-ray spectrum in coincidence with the group of particles indicated as "^{210}Po" in panel (a). (inset) Partial level scheme of ^{210}Po showing the excited states which feed the first excited 2^+ state directly. The thicknesses of the arrows (and the shown percentages) are proportional to the observed γ -ray intensities [18]. The transitions not observed in our data are presented with dashed arrows.

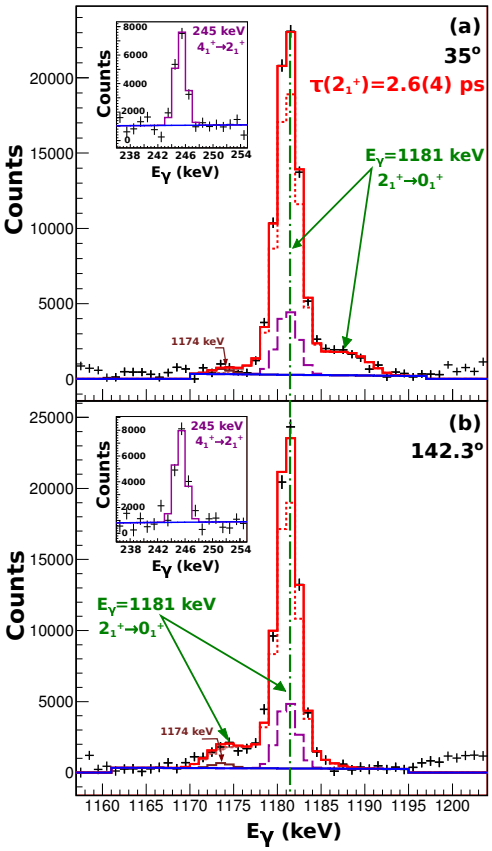

Figure 4. (Color online) Simultaneous line-shape fits of the 1181-keV ($2_1^+ \rightarrow 0_1^+$) transition observed at forward (a) and at backward (b) angles. The solid (red) line represents the total fit. The 1181-keV line is fitted simultaneously with the 245-keV ($4_1^+ \rightarrow 2_1^+$) line which is always emitted from a stopped nucleus (the insets). The dotted and dashed lines represent the individual contributions of 1181-keV (red) and 245-keV (purple) lines, respectively, to the total fit. An unidentified stopped contaminant with $E_\gamma = 1174$ keV is taken into account (brown).

The line-shape analysis was performed with the integrated software package APCAD (Analysis Program for Continuous Angle DSAM) [19]. Details about the used approach can be found in Ref. [3] where the software was verified.

The lifetime of the first excited 2^+ state of ^{210}Po was obtained from the line shape of the 1181-keV ($2_1^+ \rightarrow 0_1^+$) transition. The feeding history of the state (see the inset in Fig. 3(b)) was accounted. A special care was taken to account for the impact of the 245-keV ($4_1^+ \rightarrow 2_1^+$) transition. The 4_1^+ state of ^{210}Po is a long-lived state with lifetime $\tau = 2.21(10)$ ns [5]. Consequently, it always decays at rest in the present experiment. Indeed, as can be seen from the insets in Fig. 4 the 245-keV γ-ray line show no indication of Doppler-shifted components in its shape. Hence, when the 2_1^+ state is fed from the $4_1^+ \rightarrow 2_1^+$ transition it also always decays at rest which gives extra counts into the fully stopped component of the 1181-keV transition. In order to extract correctly the lifetime of the first 2^+ state of ^{210}Po by means of the Doppler-shift attenuation method, the contribution of the γ rays coming from the 245-keV transition to the fully stopped component of the 1181-keV transition has to be eliminated. That procedure could be automatically carried out with APCAD by simultaneously fitting the 1181- and the 245-keV lines.

Under this assumption, the final value of the lifetime of the 2_1^+ is extracted to be 2.6(4) ps. Taking into account the known electron conversion coefficient for the $2_1^+ \rightarrow 0_1^+$ transition of ^{210}Po [20], the revised lifetime of the 2_1^+ state translates to absolute transition strength $B(E2; 2_1^+ \rightarrow 0_1^+) = 136(21)$ e^{2}fm^4 = 1.83(28) Wu.

4. Discussion

The derived absolute $B(E2)$ values between the first 2^+ and ground states in both (^{212,210}Po) nuclei indicate very low collectivity. In fact, the revised value for ^{210}Po is a factor of three times larger than the adopted one but still two times smaller than the calculated one in the framework of the single-j shell model [14]. In the case of ^{212}Po, the obtained value is more than a factor of two times smaller than the calculated one in the framework of the single-j shell model [3]. The results from the single-j shell-model calculations for ^{210,212}Po and ^{210}Pb (for completeness) are presented in Table 1. The labelling of the columns reflects the approach in choosing the effective charges. In the case of SM1-gh, the effective proton and neutron charges in the $E2$ transition operator were determined from the measured $B(E2; 8_1^+ \rightarrow 6_1^+)$ values for ^{210}Pb and ^{210}Po [20] This approach yields effective charges of $e_\nu = 1.04e$ and $e_\pi = 1.52e$. Another approach is to determine the effective charges from the measured $B(E2; 2_1^+ \rightarrow 0_1^+)$ values for ^{210}Pb and ^{210}Po which leads to effective charges of e_ν=0.83e and e_π=1.09e. The results from these calculations are presented in the column labelled as SM2-

IOP Conf. Series: Journal of Physics: Conf. Series **1023** (2018) 012019 doi:10.1088/1742-6596/1023/1/012019

Table 1. Comparison between the experimental and calculated properties of the yrast states in ^{210}Po, ^{210}Pb and ^{212}Po. Except the values from this study, all other experimental $B(E2)$ values are from Ref. [20]. $B(E2)$ values are given in $e^2\text{fm}^4$.

Transition	^{210}**Po**			^{210}**Pb**			^{212}**Po**		
$J_i^\pi \to J_f^\pi$	Expt	SM1-gh	SM2-gh	Expt	SM1-gh	SM2-gh	Expt	SM1-gh	SM2-gh
$2_1^+ \to 0_1^+$	136(21)	263	137	105(30)	166	106	193(24)	464	271
$4_1^+ \to 2_1^+$	331(13)	302	157	360(68)	191	121	–	535	313
$6_1^+ \to 4_1^+$	229(7)	209	109	158(60)	132	84	293(83)	301	178
$8_1^+ \to 6_1^+$	84(3)	84	44	53(23)	53	34	173(68)	103	62

Table 2. Results from the realistic shell-model calculations (SM) for the low-lying yrast states of ^{210}Po and ^{210}Pb, and the QPM calculations for the nucleus ^{210}Po in comparison with the experimental data taken from Ref. [20]. $B(E2)$ values are given in $e^2\text{fm}^4$.

	^{210}Pb		^{210}Po				^{210}Pb		^{210}Po		
J_i^π	E_x, (MeV)		E_x, (MeV)			J_f^π	$B(E2; J_f^\pi \to J_i^\pi)$		$B(E2; J_f^\pi \to J_i^\pi)$		
	Expt	SM	Expt	SM	QPM		Expt	SM	Expt	SM	QPM
2_1^+	0.80	0.84	1.18	1.20	1.10	0_1^+	105(30)	109	136(21)	133	135
4_1^+	1.10	1.10	1.43	1.47	1.16	2_1^+	360(68)	144	331(13)	169	41
6_1^+	1.20	1.19	1.47	1.48	1.20	4_1^+	158(60)	101	227(5)	116	28
8_1^+	1.28	1.23	1.56	1.53	1.21	6_1^+	53(23)	43	83(3)	46	11

gh. The problem is evident – if the effective charges are fixed to the $B(E2; 8_1^+ \to 6_1^+)$ values (SM1-gh), the $B(E2; 2_1^+ \to 0_1^+)$ values are overestimated, otherwise, if the effective charges are fixed to the $B(E2; 2_1^+ \to 0_1^+)$ values (SM2-gh), the $B(E2; 8_1^+ \to 6_1^+)$ and the $B(E2; 6_1^+ \to 4_1^+)$ values are underestimated. This analysis suggests that agreement between experimental and simple single-j shell model cannot be achieved for the $B(E2)$ rates for ^{210,212}Po and ^{210}Pb by adjusting the effective charges.

At this point, it can be speculated that the failure of the single-j shell model originates from the extremely limited model space. To check this hypothesis we have performed realistic shell-model calculations in the cases of ^{210}Po and ^{210}Pb. The results are presented and compared to the experimental data in Table 2 and the details about these calculations are presented in [14]. The realistic shell model (SM) reproduces almost perfectly the energies of the yrast states in ^{210}Pb and ^{210}Po. However, in both cases the description of the $B(E2)$ values is only marginally improved with respect to the ones obtained in the single-j shell-model calculation (SM2-gh).

It is also interesting to check whether the problem is specific for shell models only. For this purpose we have performed Quasi-particle Phonon Model (QPM) calculations [21] for ^{210}Po. The results are presented in Table 2 and the details about these calculations can be found in [18]. The energies of the states of interest are reasonably well reproduced. It has to be noted that in the chosen approach to fix the strength parameters to the electric strengths of the 2_1^+ state, the result for the energies of the states should be considered as a prediction of the model. The major discrepancy between the QPM calculations and the experimental data appears in the $E2$ transition strengths for the cascade $8_1^+ \to 6_1^+ \to 4_1^+$. Overall, the model underestimates these values by a factor of 8. The problem existing in the shell model description also appears in a different form in the present QPM calculations.

5. Summary

In the present study we have measured the lifetimes of the 2_1^+ states of ^{212,210}Po. The derived absolute $B(E2)$ values indicate low collectivity in the structure of these states. No consistent description of the properties of the yrast 2_1^+, 4_1^+, 6_1^+ and 8_1^+ states in both nuclei is observed in the framework of nuclear shell models. The additional QPM calculations which have been done for the nucleus ^{210}Po show that the problem existing in the shell model description also appears in a different form in the QPM calculations. More thorough theoretical investigations of this problem are needed.

Acknowledgements

D.K. acknowledges the support from Deutscher Akademischer Austauschdienst. This work was supported by the partnership agreement between the University of Cologne and University of Sofia, by the BgNSF under grant DN08/23/2016, by STFC, by the German-Bulgarian exchange program under grants PPP57082997 & DNTS/01/05/2014, by the DFG under grant SFB 1245, and by the BMBF under grants 05P12RDCIB, 05P15RDFN1,9 and 05P15RDCIA.

References

[1] M.G. Mayer and J.H.D. Jensen,*Elementary Theory of Nuclear Shell Structure* (John Wiley & Sons, Inc., 1955).
[2] R.F. Casten, Phys. Lett. B **152**, 145 (1985).
[3] D. Kocheva *et al.*, Phys. Rev. C **93**, 011303(R) (2016).
[4] N. Auerbach, I. Talmi, Phys. Lett. **10**, 297 (1964).
[5] O. Häusser *et al.*, Nucl. Phys. A **273**, (1976) 253.
[6] C. Ellegaard *et al.*, Nucl. Phys. A **206**, (1973) 83.
[7] L. Coraggio *et al.*, Phys. Rev. C **60**, (1999) 064306.
[8] E. Caurier, M. Rejmund, H. Grawe, Phys. Rev. C **67**, (2003) 054310.
[9] T.K. Alexander and J.S. Forster, Adv. Nucl. Phys. **10**, 197 (1978).
[10] A.Z. Schwarzschild, E.K. Warburton, Ann. Rev. Nucl. Sci. **18**, 265 (1968).
[11] A. Dewald, O. Möller, and P. Petkov, Prog. Part. Nucl. Phys. **67**, 786 (2012).
[12] A.R. Poletti *et al.*, Nucl. Phys. A **473**, 595 (1987).
[13] A. Astier, P. Petkov, M.-G. Porquet, D.S. Delion, and P. Schuck, Phys. Rev. Lett. **104**, 042701 (2010); A. Astier, P. Petkov, M.-G. Porquet, D.S. Delion, and P. Schuck, Eur. Phys. J. A **46**, 165 (2010).
[14] D. Kocheva *et al.*, Phys. Rev. C **96**, 044305 (2017)
[15] A. Dewald, S. Harissopulos and P. von Brentano, Z. Phys. A**334**, 163 (1989).
[16] G. Böhm, A. Dewald, P. Petkov and P. von Brentano, Nucl. Inst. Meth. A**329**, 248 (1993).
[17] L. G. Mann *et al.*, Phys. Rev. C **38**, (1988) 74.
[18] D. Kocheva *et al.*, Eur. Phys. J. A **53**, 175 (2017)
[19] C. Stahl, J. Leske, M. Lettmann, N. Pietralla, Comp. Phys. Com. **214**, (2017) 174.
[20] M. Shamsuzzoha Basunia, Nucl. Data Sheets **121**, (2014) 561.
[21] V. G. Soloviev, Theory of Atomic Nuclei, Quasiparticles and Phonons (IOP, London, 1992).